Targeted enrichment outperforms other enrichment techniques and enables more multi-species RNA-Seq analyses

Matthew Chung[1,2], Laura Teigen[3], Hong Liu[4], Silvia Libro[5], Amol Shetty[1], Nikhil Kumar[1], Xuechu Zhao[1], Robin E. Bromley[1], Luke J. Tallon[1], Lisa Sadzewicz[1], Claire M. Fraser[1,6], David A. Rasko[1, 2], Scott G. Filler[4,7], Jeremy M. Foster[5], Michelle L. Michalski[3], Vincent M. Bruno [1, 2], Julie C. Dunning Hotopp[1,2,8]

[1]Institute for Genome Sciences, University of Maryland School of Medicine, Baltimore, MD 21201, USA

[2]Department of Microbiology and Immunology, University of Maryland School of Medicine, Baltimore, MD 21201, USA

[3]University of Wisconsin Oshkosh, Oshkosh, WI 54901, USA

[4]Division of Infectious Diseases, Los Angeles Biomedical Research Institute, Harbor-UCLA Medical Center, Torrance, California 90502, USA.

[5]New England Biolabs, Ipswich, MA 01938, USA.

[6]Department of Medicine, University of Maryland School of Medicine, Baltimore, MD 21201, USA.

[7]David Geffen School of Medicine at UCLA, Los Angeles, California 90502, USA.

[8]Greenebaum Cancer Center, University of Maryland, Baltimore, MD 21201, USA

MC: mattchung@umaryland.edu

LT: lauraeteigen@gmail.com

HL: hliu@labiomed.org

SL: libro@neb.com

AS: ashetty@som.umaryland.edu

NK: nkumar29@gmail.com

XZ: xuzhao@som.umaryland.edu

REB: rbromley@som.umaryland.edu

LJT: ljtallon@som.umaryland.edu

LS: lsadzewicz@som.umaryland.edu

CMF: cmfraser@som.umaryland.edu

DAR: drasko@som.umaryland.edu

SGF: sfiller@ucla.edu

JMF: foster@neb.com

MLM: michalsk@uwosh.edu

VMB: bvincent@som.umaryland.edu

JCDH: jdhotopp@som.umaryland.edu

Abstract

Enrichment methodologies enable analysis of minor members in multi-species transcriptomic analyses. We compared standard enrichment of bacterial and eukaryotic mRNA to targeted enrichment with Agilent SureSelect (AgSS) capture for *Brugia malayi*, *Aspergillus fumigatus,* and the *Wolbachia* endosymbiont of *B. malayi* (*w*Bm). Without introducing significant systematic bias, the AgSS quantitatively enriched samples, resulting in more reads mapping to the target organism. The AgSS-enriched libraries consistently had a positive linear correlation with its unenriched counterpart (r^2=0.559-0.867). Up to a 2,242-fold enrichment of RNA from the target organism was obtained following a power law (r^2=0.90), with the greatest fold enrichment achieved in samples with the largest ratio difference between the major and minor members. While using a single total library for prokaryote and eukaryote in a single sample could be beneficial for samples where RNA is limiting, we observed a decrease in reads mapping to protein coding genes and an increase of multi-mapping reads to rRNAs in AgSS enrichments from eukaryotic total RNA libraries as opposed to eukaryotic poly(A)-enriched libraries. Our results support a recommendation of using Agilent SureSelect targeted enrichment on poly(A)-enriched libraries for eukaryotic captures and total RNA libraries for prokaryotic captures to increase the robustness of multi-species transcriptomic studies.

Introduction

Dual species transcriptomic experiments have been increasingly employed as a method to analyze the transcriptomes of multiple species within a system[1-9]. However, obtaining a sufficient quantity of reads from each organism is a major issue when simultaneously analyzing the transcriptomes of multiple organisms within a single sample. When extracting total RNA from a host sample, the signal from host transcripts typically overwhelms the signal from secondary organism transcripts under most biologically meaningful conditions. Differential enrichments have been designed to physically extract RNA from secondary organisms in samples by depleting the highly abundant rRNAs and selecting transcripts based on differing properties between the two organisms, such as the differential poly-adenylation status of transcripts [10]. However, in eukaryote-eukaryote dual species transcriptomics experiments, these differences are often not present. Additionally, methods used to enrich for prokaryotic RNA from samples dominated by eukaryotic RNA can fail when the poly(A)-depletion method is unable to remove eukaryotic long non-coding RNAs that lack 3'-polyadenylatation, and when the efficacy of rRNA depletion is low, as observed with some organisms.

The Agilent SureSelect platform serves as a hybridization-based enrichment method that uses specific baits to target transcripts of interest (www.genomics.agilent.com). By designing sequence-specific baits for an organism, it becomes possible to extract transcripts of interest, such as mRNAs, while avoiding unwanted RNA types, such as rRNAs and tRNAs. In dual species transcriptomics, one of the main advantages of the Agilent SureSelect system is the ability to extract reads in systems where an organism has low relative abundance [11]. To test the efficacy of the Agilent SureSelect platform on multiple dual- and tripartite-species systems where insufficient numbers of reads are obtained from the minor member(s), we designed Agilent SureSelect baits for: (1) *Brugia malayi*, a filarial nematode and the causative agent of lymphatic filariasis, (2) *w*Bm, the obligate mutualistic *Wolbachia* endosymbiont of *B.*

malayi and (3) *Aspergillus fumigatus* AF293, a fungal pathogen known to cause aspergillosis in immunocompromised individuals.

In filarial nematode transcriptomics, it is relatively straightforward to isolate nematode samples from the mammalian/definitive host while minimizing contaminating host material. Therefore, the *Brugia* transcriptome can be easily obtained from poly(A)-enriched RNA from *Brugia* samples originating from the mammalian definitive host, which is often an experimentally infected gerbil (*Meriones unguiculatus*). However, sampling the *Wolbachia* endosymbiont transcriptome in these worms is problematic because the endosymbionts contribute less RNA to the total RNA pool. Therefore, *w*Bm reads are overwhelmed by *B. malayi* reads and must be enriched using a rRNA- and poly(A)-depletion. In the mosquito vector host, the parasitic worms develop in the thoracic muscles where they are not easily isolated. Therefore, whole infected mosquito thoraces containing the larval *B. malayi* are used for RNA isolation. As such the *B. malayi* reads are overwhelmed by reads from those of the mosquito vector, typically experimentally infected *Aedes aegypti*, and the reads of endogenous *w*Bm are even further dwarfed compared to samples obtained from the definitive host. In a separate dual-species transcriptomics experiment examining *A fumigatus* infections, *A. fumigatus* reads are overwhelmed by reads from the human or mouse host making it difficult to analyze the fungal transcriptome in this host-pathogen interaction. For each eukaryotic system, the performance of the poly(A)-enrichment was compared to that of poly(A)-enrichment supplemented with the Agilent SureSelect platform in extracting *B. malayi* and *A. fumigatus* reads. Additionally, the efficacy of the Agilent SureSelect platform in extracting prokaryotic reads was determined by comparing the total RNA Agilent SureSelect capture to the RiboZero-treated, poly(A)-depletion method in extracting *w*Bm reads.

Methods

Mosquito preparation

Aedes aegypti black-eyed Liverpool strain mosquitoes were obtained from the NIH/NIAID Filariasis Research Reagent Resource Center (FR3) and maintained in the biosafety level 2 insectary at the University of Wisconsin Oshkosh (UWO). Desiccated mosquito eggs were hatched in deoxygenated water and the larvae maintained on a slurry of ground TetraMin fish food (Blacksburg, VA, USA) at 27 °C and 80% relative humidity. Female pupae were separated from males using a commercial larval pupal separator (The John Hock Company, Gainesville, FL, USA) and maintained on cotton pads soaked in sucrose solution. Adult female mosquitos were deprived of sucrose ~8 h prior to blood feeding. Mosquitoes were infected with the *B. malayi* FR3 strain by feeding on microfilaremic cat blood (FR3) through parafilm via a glass jacketed artificial membrane feeder. Microfilaremic cat blood was diluted with uninfected rabbit blood to achieve a suitable parasite density for infection (100-250 mf (microfilariae)/20 µL) and mosquitoes were allowed to feed to repletion. Mosquitoes were maintained in insect incubators until time of worm harvest.

Nematode preparation

To examine larval development in the vector, groups of mosquitoes were sampled at 18 h post infection (hpi), 4 days post infection (dpi), and 8 dpi. Because larval development occurs in the thoracic muscle of the mosquito, thoraces of infected mosquitoes containing larval *B. malayi* were separated from the head, abdomen, legs, and wings; flash frozen in liquid nitrogen; and stored at -80 °C prior to RNA isolation. To generate third stage larvae (L3) of *Brugia malayi,* infected mosquitoes at 9-16 dpi were processed in bulk using the NIAID/NIH Filariasis Research Reagent Resource Center (FR3) Research Protocol 8.4 (www.filariasiscenter.org). Larvae were isolated in RPMI media containing 0.4 U penicillin and 4 µg streptomycin per mL (RPMI + P/S), flash frozen in liquid nitrogen, and stored at -80 °C. To generate fourth larval stages (L4) and adult worms, freshly isolated L3s were injected into the peritoneal

cavities of Mongolian gerbils (*Meriones unguiculatus*). Briefly, male Mongolian gerbils three months of age or older (Charles River, Wilmington, MA, USA) were anesthetized with 5% isoflurane, immobilized on a thermal support, and administered ocular Paralube. The inguinal region for each gerbil was shaved and disinfected with iodine. Infections were performed by delivering L3 larvae into the peritoneal cavity using a butterfly catheter, which was left in place and flushed afterwards with 1 mL warmed RPMI + P/S to ensure delivery of all larvae. Afterwards, gerbils were removed from the plane of anesthesia and allowed to fully recover in a hospital cage prior to returning to group housing. Worms were later harvested by euthanizing the gerbils and soaking the peritoneal cavities in warm RPMI + P/S. Worms were washed in warm RPMI +P/S to remove traces of gerbil tissue and flash frozen with liquid nitrogen and stored at -80 °C. All animal care and use protocols were carried out in accordance with the relevant guidelines and regulations and were approved by the UWO IACUC.

Mosquito/Nematode/*Wolbachia* RNA isolation

Mosquito thoraces were combined with TRIzol (Zymo Research, Irvine, CA, USA) at a ratio of 1 mL TRIzol per 50-100 mg mosquito tissue while nematode samples were processed using a 3:1 volume ratio of TRIzol to sample. β-mercaptoethanol was added to a final concentration of 0.1%. The tissues were homogenized in a TissueLyser (Qiagen, Germantown, MD) at 50 Hz for 5 min. The homogenate was transferred to a new tube and centrifuged at 12,000 x g for 10 min at 4 °C. After incubating at room temperature for 5 min, 0.2 volumes of chloroform were added. The samples were shaken by hand for 15 s, incubated at room temperature for 3 min, then loaded into a pre-spun, phase lock gel heavy tube (5Prime, Gaithersburg, MD, USA) and centrifuged for 5 min at 12,000 x g at 4 °C. The upper phase was removed to a new tube and one volume of 100% ethanol was added prior to loading onto a PureLink RNA Mini column (Ambion, Austin, TX). The samples were then processed following manufacturer instructions, quantified using a Qubit fluorometer (Qiagen, Germantown, MD, USA) and/or a NanoDrop spectrometer (NanoDrop, Wilmington, DE, USA). The RNA was then shipped on dry ice to the University

of Maryland where it was treated with the TURBO DNA-*free* kit (Ambion, ThermoFisher Scientific, Waltham, MA, USA) according to the manufacturer's protocol.

A. fumigatus infection

Two different models of invasive aspergillosis, both using male BALB/c mice, were employed [12, 13]. In the non-neutropenic model, the mice were immunosuppressed with 5 doses of cortisone acetate, with 500 mg/kg administered subcutaneously every other day four days pre-infection. In the leukopenic model, the mice were administered cyclophosphamide, 250 mg/kg intraperitoneally, and cortisone acetate, 250 mg/kg subcutaneously, on two days pre-infection. On day 4 after infection, the mice were given a second dose of cyclophosphamide, 200 mg/kg intraperitoneally, and cortisone acetate, 250 mg/kg subcutaneously. All mice were infected by placing them in a chamber containing an aerosol of *A. fumigatus* conidia for 1 h. On days 2 and 4 for the non-neutropenic model and on days 4 and 7 for the leukopenic model, 3 mice per time point were sacrificed, after which their lungs were harvested and stored in RNAlater (Ambion, ThermoFisher Scientific, Waltham, MA, USA) for subsequent RNA isolation.

A. fumigatus RNA isolation

Each lung sample was placed in a lysing matrix C tube (MP Biomedicals, Santa Ana, CA, USA) with a single 0.25 inch diameter ceramic sphere (MP Biomedicals, Santa Ana, CA, USA) and homogenized with a bead beater (FastPrep FP120, Qbiogene, Montreal, Quebec, Canada).The RNA was isolated using the RiboPure kit (Ambion, ThermoFisher Scientific, Waltham, MA, USA) following the manufacturer's instructions, treated with DNase I (ThermoFisher Scientific, Waltham, MA, USA), and purified using the RNA clean & concentrator kit (Zymo Research, Irvine, CA, USA).

Illumina NEBNext Ultra Directional RNA libraries without capture

Whole transcriptome libraries were constructed for sequencing on the Illumina platform using the NEBNext Ultra Directional RNA Library Prep Kit (New England Biolabs, Ipswich, MA, USA). When targeting eukaryotic mRNA, polyadenylated RNA was isolated using the NEBNext Poly(A) mRNA

magnetic isolation module. When targeting bacterial mRNA, samples underwent rRNA- and poly(A)-reductions, as previously described [10, 14]. SPRIselect reagent (Beckman Coulter Genomics, Danvers, MA, USA) was used to purify cDNA between enzymatic reactions and perform size selection. For indexing, the PCR amplification step was performed with primers containing a 7-nt index sequence. Libraries were evaluated using the GX touch capillary electrophoresis system (Perkin Elmer, Waltham, MA) and sequenced on a HiSeq2500 generating 100-bp paired end reads.

Wolbachia custom RNA capture

Pre-capture libraries were constructed from 500-1000 ng of total RNA samples using NEBNext Ultra Directional RNA Library Prep kit (NEB, Ipswich, MA, USA). First strand cDNA was synthesized without mRNA extraction to retain non-polyadenylated transcripts and was fragmented at 94 ^{o}C for 8 min. After adaptor ligation, cDNA fragments were amplified with 10 cycles of PCR before capture. *Wolbachia* transcripts were captured from 200 ng of the amplified libraries using an Agilent SureSelectXT RNA (0.5-2 Mbp) bait library designed specifically for *w*Bm. Library-bait hybridization reactions were incubated at 65 C for 24 h then bound to MyOne Streptavidin T1 dynabeads (Invitrogen, Carlsbad, CA, USA). After multiple washes, bead-bound captured library fragments were amplified with 18 cycles of PCR. The libraries were loaded on a HiSeq4000 generating 151-bp paired end reads.

B. malayi custom RNA capture

Pre-capture libraries were constructed from 1000 ng of total RNA samples using NEBNext Ultra Directional RNA Library Prep kit (NEB #E7420, Ipswich, MA, USA). Except where noted, poly(A)-enrichment according to the manufacturer's protocol was used. In comparisons of capture on poly(A)-enriched libraries with total RNA libraries, total RNA libraries were constructed after first strand cDNA was synthesized without mRNA extraction to retain non-polyadenylated transcripts and fragmented at 94 ^{o}C for 8 min. After adaptor ligation, cDNA fragments were amplified for 10 cycles of PCR before capture. *B. malayi* transcripts were captured from 200 ng of the amplified libraries using an Agilent

SureSelectXT Custom (12-24 Mbp) bait library designed specifically for *B. malayi*. Library-bait hybridization reactions were incubated at 65 °C for 24 h then bound to MyOne Streptavidin T1 Dynabeads (Invitrogen, Carlsbad, CA). After multiple rounds of washes, bead-bound captured library fragments were amplified with 16 cycles of PCR. The libraries were loaded on a HiSeq4000 generating 151-bp paired end reads.

Aspergillus custom RNA capture

Pre-capture libraries were constructed from 700 ng of total RNA samples using NEBNext Ultra Directional RNA Library Prep kit (NEB #E7420, Ipswich, MA, USA) according to the manufacturer's protocol. Briefly, mRNA was extracted with oligo-d(T) beads and reverse-transcribed into first strand cDNA with random primers. First strand cDNA was fragmented at 94 °C for 8 min. After adaptor ligation, cDNA fragments were amplified in thermocycler for 10 cycles before capture. *Aspergillus* transcripts were captured from 100 ng of amplified libraries Agilent SureSelectXT Custom (12-24 Mbp) bait library for *A. fumigatus*. Libraries were incubated at 65 °C for 24 h then bound to MyOne Streptavidin T1 Dynabeads (Invitrogen, Carlsbad, CA, USA). After multiple rounds of washes, bead-bound captured library fragments were amplified with 16 cycles of PCR. The libraries were loaded on a HiSeq4000 generating 151-bp paired end reads.

Sequence alignment, feature counts, and fold enrichment calculations

The sequence reads originating from all samples used in all *B. malayi* and *A. fumigatus* AF293 comparisons were mapped to the *B. malayi* genome WS259 (www.wormbase.org) or *A. fumigatus* AF293 genome CADRE34 (www.aspergillusgenome.org), respectively, using the TopHat v1.4 [15] aligner. Read counts for all genes were obtained using HTSeq (v0.5.3p9) [16], with the mode set to "union." For the *B. malayi* genome, RNAmmer v1.2 [17] identified 5 protein-coding genes (WBGene00228061, WBGene00268654, WBGene00268655, WBGene00268656, WBGene00268657) overlapping with predicted rRNAs. Reads overlapping with these genes were excluded from all gene-based analyses.

The sequencing reads for the *w*Bm comparisons were mapped to the *w*Bm assembly [18] using Bowtie v0.12.9 [19]. Counts for each *w*Bm gene were calculated by summing the sequencing depth per base pair, obtained using the DEPTH function of SAMtools v1.1 [20], for each of the unique genomic positions in each gene. This value was then divided by the average read length for the sample, yielding a read count value for each gene. Across all comparisons, read counts were normalized between each of the different samples through a conversion to transcripts per million (TPM).

The fold enrichment, F_e , of reads belonging to an organism conferred by the Agilent SureSelect compared to the other enrichment techniques was calculated as

$$F_e = \left(\frac{M_{AGSS}}{S_{AGSS}}\right) / \left(\frac{M_{poly(A)}}{S_{poly(A)}}\right)$$

the ratio of the number of reads mapped with Agilent SureSelect capture (M_{AGSS}) to the number of reads sequenced with Agilent SureSelect capture (S_{AGSS}) divided by the ratio of number of reads mapped with poly(A)-enrichment or the rRNA-, poly(A)-depletion ($M_{poly(A)}$) to the number of reads sequenced with poly(A)-enrichemnt or the rRNA-, poly(A)-depletion ($S_{poly(A)}$). By taking a ratio of the percentage of mapped reads for each enrichment technique, the fold enrichment value represents an amount of enrichment conferred by the Agilent SureSelect when compared to the other enrichment technique for a given sample. The fold enrichment values when comparing the efficacy of Agilent SureSelect capture on poly(A)-enriched libraries to total RNA libraries were calculated similarly as

$$F_e = \left(\frac{M_{AGSS-poly(A)}}{S_{AGSS-poly(A)}}\right) / \left(\frac{M_{AGSS-total\ RNA}}{S_{AGSS-total\ RNA}}\right)$$

where $M_{AGSS-poly(A)}$ and $S_{AGSS-poly(A)}$ represent the mapped and sequenced reads from poly(A)-enriched Agilent SureSelect capture libraries, while $M_{AGSS-total\ RNA}$ and $S_{AGSS-total\ RNA}$ represent the mapped and sequencing reads from Agilent SureSelect capture from the total RNA libraries.

Results

Comparison of poly(A)-enriched Agilent SureSelect to only poly(A)-enrichment for *B. malayi*

Poly(A)-enriched, Agilent SureSelect libraries were compared to only poly(A)-enriched libraries from six RNA samples originating from three different time points of the *B. malayi* vector life stages (18 hpi, 4 dpi, and 8 dpi) **(Figure 1a)**. Across these six samples, the poly(A)-enrichment alone yielded 0.38-23.35% of reads mapping to the *B. malayi* genome, with 61.25-82.51% of reads mapping to the *A. aegypti* genome. Of the poly(A)-enriched libraries capture using the Agilent SureSelect baits, 56.14%-81.52% of reads mapped to the *B. malayi* genome, with 2.28-24.02% of reads mapping to the *A. aegypti* genome **(Supplementary Table 1)**. The fold enrichment conferred to libraries captured with Agilent SureSelect was found to be inversely proportional to the number of reads mapped to its poly(A)-enrichment only counterpart, such that experiments with the fewest reads mapped in the poly(A)-enrichment had the highest fold enrichment with the Agilent SureSelect capture. The 18 hpi samples, which have the lowest percentage of mapped reads to the *B. malayi* genome has the greatest fold enrichment (110-146x) while the 8 dpi samples, with the highest percentage of *B. malayi* mapped reads, has the lowest fold enrichment (3-4x).

A principal component analysis (PCA) using the $\log_2$-TPM values for the 11,085 predicted *B. malayi* protein-coding genes reveals that the *B. malayi* samples cluster based on life stage rather than library preparation **(Figure 2a)**, suggesting that the capture does not introduce a systematic bias to the transcriptome of a sample. The exceptions are the 18 hpi vector poly(A)-enrichment-only samples, which we attribute to these samples having an insufficient number of reads mapped to features (143,078 and 212,342 reads, accounting for <20 reads per gene assuming equal distribution) to accurately represent the transcriptome. Supporting this, in the 18 hpi samples, an average of 2,460 protein coding genes (22.18% of the *B. malayi* protein coding genes) had reads mapping to them in the poly(A)-enriched Agilent SureSelect samples but not its poly(A)-enriched counterpart, while in the 4 dpi and 8 dpi samples, an average of 952 (8.58%) and 566 (5.09%) genes, respectively, had reads mapping to

them from the poly(A)-enriched Agilent SureSelect libraries but not the poly(A)-enriched libraries. Collectively, across all 6 samples, 392 unique genes were detected in only the poly(A)-enrichment, but not the poly(A)-enriched Agilent SureSelect libraries in at least one comparison. The Agilent SureSelect probe design was based on an older version of the annotation compared to the version used for feature calling, and as such, 91 of these 392 genes were not covered by a probe.

The $\log_2$ TPM values from the poly(A)-enriched Agilent SureSelect and the poly(A)-enriched libraries had a positive linear correlation with r^2 values ranging from 0.559-0.867 **(Figure 2b)**. The 4 dpi and 8 dpi correlations were the strongest **(Figure 2b)**, for the reasons discussed above, namely that fewer reads were recovered from the 18 hpi vector samples without Agilent SureSelect enrichment. To identify individual genes in which the library preparations affected the calculated TPM, the $\log_2$ ratio of the poly(A)-enriched Agilent SureSelect TPM relative to the poly(A) enrichment TPM for each gene was calculated (**Figure 2c**). Genes with relatively similar expression levels in the two library preparations would have a $\log_2$ ratio of 0 while genes more highly expressed in the poly(A)-enriched Agilent SureSelect preparation would be >0 and genes more highly expressed in the poly(A) enrichment would be <0. Genes with a $\log_2$-ratio value of >3 standard deviations from the mean were defined as having significantly altered levels of expression between the two libraries. Across all six comparisons, the number of genes with significantly higher TPM values in the Agilent SureSelect libraries never accounted for >0.31% (<34 genes) of all protein-coding genes in the *B. malayi* genome. The number of genes with significantly higher TPM values in the poly(A)-enrichment ranged from 0.93%-1.52% (103-168 genes) of all protein-coding genes in *B. malayi* across the six comparisons **(Supplementary Table 1)**.

Comparison of poly(A)-enriched Agilent SureSelect and only poly(A)-enrichment for *A. fumigatus*

The *A. fumigatus* AF293 transcriptome from poly(A)-enriched Agilent SureSelect and poly(A)-enriched only libraries were compared for 11 RNA samples from immunocompromised mice or neutropenic mice

283 infected with *A. fumigatus* AF293 **(Figure 1a)**. Of the 11 samples, 6 samples originated from three
284 replicates of immunocompromised mice taken 2 dpi and 4 dpi with *A. fumigatus*. The remaining 5
285 samples consist of two replicates of neutropenic mice taken 4 dpi with *A. fumigatus* and three replicates
286 of neutropenic mice taken 7 dpi with *A. fumigatus*.
287 Across all 11 samples, the total percentage of reads mapping to *A. fumigatus* from the poly(A)-enriched
288 samples was consistently ≤0.02%, while 0.30%-11.74% of reads mapped in the poly(A)-enriched Agilent
289 SureSelect samples. In the poly(A)-enrichment only samples, a maximum of 27,531 reads mapped to *A.*
290 *fumigatus* AF293, accounting for <3 reads/gene if they were evenly distributed. As such, comparisons
291 between Agilent SureSelect and poly(A)-enriched libraries are not possible.
292 There are 4,168-7,387 genes (41.68%-76.70%) that are identified only in the poly(A)-enriched Agilent
293 SureSelect libraries but not the poly(A)-enriched libraries, compared to the maximum of 52 genes
294 identified only in the poly(A)-enriched libraries across all *A. fumigatus* comparisons **(Supplementary**
295 **Table 2)**. For all 11 comparisons, using the Agilent SureSelect methodology conferred a 614x to 1,212x
296 fold enrichment of *A. fumigatus* AF293 reads relative to the poly(A)-enrichment, demonstrating the
297 power of this technology in dual-species transcriptomics, going from data that was unamenable to a
298 traditional transcriptomics analysis to obtaining data where robust statistical tests can be performed.
299 The proportion of reads mapping to features relative to the total number of reads mapped is consistent
300 between samples of the same library preparation, with *A. fumigatus* poly(A)-enriched Agilent SureSelect
301 samples ranging from 52.23-54.87% and the poly(A)-enrichment samples ranging from 45.89-51.22%.

302 ## Comparison of total RNA Agilent SureSelect to rRNA-, poly(A)-depleted for the
303 ## bacterial *Wolbachia* endosymbiont *w*Bm

304 With both of the previously discussed biological systems, we tested the effectiveness of the Agilent
305 SureSelect platform to study eukaryote-eukaryote host-pathogen interactions. By enriching for *w*Bm
306 reads in *B. malayi* samples, we sought to test the effectiveness of Agilent SureSelect libraries in

extracting prokaryotic reads. The standard protocol for Agilent SureSelect capture in eukaryotes relies on capturing targets from poly(A)-enriched libraries, but for prokaryotic samples the capture is performed on total RNA libraries. These total RNA Agilent SureSelect libraries were compared to rRNA-, poly(A)-depleted library preparations from nine *B. malayi* samples taken at various stages of the life cycle to analyze the transcriptome of its *Wolbachia* endosymbiont, *w*Bm **(Figure 1b)**. Three RNA samples were obtained from the mammalian portion of the *Brugia* lifecycle where worms are large enough to be physically separated from the mammalian tissue. These RNA samples generate predominantly *Brugia* reads with a minority of *Wolbachia* reads. Of these three samples, one sample was recovered at 24 dpi, representative of female worms just prior to the final L4 to adult molt, while the other two samples are from two reproductively mature adult females recovered 7 months post-infection. The other six samples are from the vector portion of the *B. malayi* lifecycle where tripartite RNA samples are obtained, consisting of predominantly mosquito reads, with a smaller percentage of *Brugia* reads, and an even smaller percentage of *Wolbachia* reads. These six samples consisted of two *A. aegypti* replicates each of the 18 hpi, 4 dpi, and 8 dpi with *B. malayi*, representative of the L1 through early L3 *B. malayi* life stages. Of the six samples taken from the vector life stages, at most 1,552 reads (<0.01% of sequenced reads) mapped to the *w*Bm genome from the rRNA-, poly(A)-depleted samples, of which 729 reads were identified as mapping to protein-coding genes for an average of <1 read mapped/gene **(Supplementary Table 3)**. In contrast, the rRNA-, poly(A) depleted adult female *B. malayi* samples taken from the mammalian host had a minimum of 17,107 reads mapping to *w*Bm protein-coding genes, equating to ~20 reads/gene while the 24 dpi sample had 246,549 reads mapped to protein-coding genes, equating to ~294 reads/gene.

The Agilent SureSelect-enriched samples had an increased number of *w*Bm-mapping reads for all 9 samples, with 20.4-37.4 million reads (18.68%-32.53%) mapping to *w*Bm genes for the three gerbil samples and 0.2-4.0 million reads (0.46-6.43% of sequenced reads) mapping to *w*Bm genes for the

mosquito vector samples. The total RNA Agilent SureSelect libraries from gerbil samples were 20-41x fold enriched for *w*Bm reads relative to the rRNA-, poly(A)-depleted libraries while the libraries from vector samples were 353-2,242x fold enriched. The proportion of *w*Bm reads mapped to protein-coding genes were consistently higher in the Agilent SureSelect in both the gerbil and vector samples, ranging from 88.31-92.44% and 44.34-56.14%, respectively, compared to the 10.62-20.11% and 45.21-58.73% observed in the rRNA-, poly(A)-depleted samples. This difference in the number of *w*Bm reads mapping to protein-coding genes can be partially attributed to a greater number of reads mapping to rRNAs in the rRNA-, poly(A)-depleted samples, with 18.73-33.82% of *w*Bm mapped reads mapping to rRNAs compared to 0.1-2.1% observed in the total RNA, Agilent SureSelect samples **(Supplementary Table 3)**.

A principal component analysis using the TPM values of the three gerbil life stage comparisons demonstrates that individual samples segregate based on library preparation (**Figure 3a**). All three of the total RNA Agilent SureSelect samples are clustered close together, while the rRNA-, poly(A)-depleted samples are further distributed, likely due to the insufficient coverage of the *w*Bm transcriptome in the absence of Agilent SureSelect enrichment. The mosquito vector life stage samples were not used for the principal component analysis due to an insufficient number of reads mapping in the poly(A)-depletion portion of the comparison to compare the two enrichment methods. Like the *B. malayi* comparisons, the $\log_2$ TPM values from the *w*Bm Agilent SureSelect libraries and the rRNA- and poly(A)-depletion libraries made from mammalian life stages had a positive linear correlation with r^2 values ranging from 0.575-0.744 (**Figure 3b**).

A total of 45 unique genes (~5.4% of protein-coding genes in *w*Bm) were detected in at least one of the three gerbil comparisons in the sample treated using the rRNA-, poly(A)-depletion libraries but not its total RNA Agilent SureSelect counterpart. Of these 45 genes, 41 were not covered by any of the Agilent SureSelect probes while the remaining four genes had <11% of their length covered by a probe. To identify genes with significantly greater expression in one enrichment method over the other, a cutoff of

two standard deviations from the $\log_2$ ratio of the Agilent SureSelect TPM to the rRNA-, poly(A)-depleted TPM was used (**Figure 3c**). Genes with a $\log_2$ ratio of >2 standard deviations below the average $\log_2$ ratio were determined to have significantly higher expression in the rRNA-, poly(A)-depletion sample while genes with a $\log_2$ ratio >2 standard deviations above the average, were identified as having significantly higher expression in the total RNA Agilent SureSelect sample. Across the three comparisons, a total of 30 unique genes had TPM values significantly higher in the rRNA-, poly(A)-depleted sample compared to the Agilent SureSelect sample in at least one comparison. Of these genes, 17 genes were not covered by any probe, six genes had <17% of their length covered by a probe, and the remaining seven genes are covered in the entirety of their length by the probe design. Additionally, there were 152 unique genes (~18.1% of protein-coding genes in *w*Bm) detected in the total RNA, Agilent SureSelect but not the poly(A)-depletion in at least one of the comparisons. Of the 152 genes, 114 had average TPM values in the bottom quartile of the expressed genes across the three Agilent SureSelect samples, highlighting the ability of the Agilent SureSelect preparation to detect low abundance transcripts.

Comparison of Agilent SureSelect *B. malayi* transcriptome data from total RNA and poly(A)-enriched samples

For eukaryote transcriptome experiments, the Agilent SureSelect platform is typically preceded by construction of a poly(A)-selected library that is then hybridized to the bait probes. The poly(A)-enrichment step serves to remove high abundance, non-mRNA transcripts, such as rRNAs, tRNAs, and other ncRNAs. For bacterial samples, libraries must be constructed on total RNA since bacterial mRNAs lack the poly(A) tails present in eukaryotes. For eukaryote-prokaryote transcriptomic experiments, it may be advantageous to use the Agilent SureSelect platform for both bacteria and eukaryotes on the same single library constructed from total RNA, especially for clinical samples where RNA may be limiting. Therefore, we sought to compare the Agilent SureSelect enrichment on a library constructed

from total *B. malayi* RNA with one constructed following poly(A)-enrichment using two samples taken from the mosquito vector portion of the *B. malayi* life stages at 18 hpi and 8 dpi **(Figure 1c)**. For both the 18 hpi and 8 dpi timepoints, most genes yield comparable $\log_2$ TPM values between the two enrichment methods **(Figure 4a)** with <1.5% of genes having a bias towards a particular library construction protocol **(Figure 4b).** However, despite the 8 dpi comparison yielding a similar number of genes detected unique to each enrichment method, in the 18 hpi sample comparison, 1,033 genes (9.3% of all protein-coding genes) were detected only in the Agilent SureSelect, poly(A)-enriched library while 323 (2.91%) were only detected with the Agilent SureSelect, total RNA library **(Supplementary Table 4)**. In both cases, a majority of the genes detected in only one library construction method were within the bottom 20% of expressed genes in the sequencing data collected, with 815 genes (78.9%) in the selection conducted with the total RNA library and 233 genes (72.14%) in the selection conducted with the poly(A)-enriched library. Similarly, in the 8 dpi sample comparison, 2.35% (261 genes) of *B. malayi* protein-coding genes were identified only in the target captured poly(A)-enriched library while 1.71% (189 genes) were identified only in the target captured total RNA library. Again, in both cases, a majority of the genes detected in only one library construction method were within the bottom 20% of expressed genes in the sequencing data collected, with 236 genes (90.42%) in the selection conducted with the poly(A)-enriched RNA library and with 179 genes (94.71%) in the selection conducted with the total RNA library. Based off these results, both Agilent SureSelect methods can detect low abundance transcripts, but the poly(A)-enriched Agilent SureSelect was able to select for a greater number of these transcripts in both comparisons.

The percentage of reads mapping to the *B. malayi* genome were greater in the poly(A)-enriched Agilent SureSelect samples compared to the total RNA Agilent SureSelect samples, with 56.14% and 80.13% of reads mapping to the *B. malayi* genome, compared to 22.96% and 69.84%, of reads mapped for the 18 hpi and 8 dpi samples respectively. The poly(A)-enriched Agilent SureSelect samples were enriched for

reads mapping to *B. malayi* by 2.4x for the 18 hpi sample and 1.1x for the 8 dpi sample relative to the total RNA Agilent SureSelect. Additionally, in the 18 hpi and 8 dpi poly(A)-enriched RNA, Agilent SureSelect samples, 46.63% and 46.35% of their mapped reads mapped to protein-coding genes while in the total RNA Agilent SureSelect only 20.22% and 32.21% mapped to protein-coding genes **(Supplementary Table 4)**. This is explained by the increased number of multi-mapping reads observed in the total RNA Agilent SureSelect samples, with 70.29% and 39.29% of the total number of mapped reads in the 18 hpi and 8 dpi vector samples multi-mapping to the *B. malayi* genome. In comparison, only 5.93% and 5.42% of mapped reads were multi-mapping in the 18 hpi and 8 dpi poly(A)-enriched Agilent SureSelect samples. A total of 80.82% and 69.86% of these multi-mapping reads in the total RNA Agilent SureSelect 18 hpi and 8 dpi vector samples were found to be mapping to the *B. malayi* rRNAs compared to only 13.76% and 1.56% in the poly(A)-enriched Agilent SureSelect samples **(Supplementary Table 4)**. The Agilent SureSelect platform on poly(A)-enriched RNA was able to obtain both a higher percentage of *B. malayi* mapped reads and a higher percentage of *B. malayi* reads mapping to protein-coding genes. Therefore, we recommend the use of the Agilent SureSelect enrichment on poly(A)-enriched libraries for eukaryotic systems whenever possible.

Discussion

With multi-species RNA-Seq experiments emerging at the forefront of experimental designs for transcriptome analyses, novel methods are being developed to more efficiently extract the transcriptomes for multiple organisms from a single sample. By comparing the transcriptomes generated with standard enrichment methods, such as poly(A)-enrichment or rRNA-, poly(A)-depletion, against the Agilent SureSelect platform, we sought to independently validate the use of the Agilent SureSelect in enriching for transcripts originating from a specific organism of interest while minimizing any type of library bias on the transcriptome. When analyzing the *B. malayi* transcriptomes of samples prepared with or without the Agilent SureSelect, most genes could be detected using both library preparations. However, the samples prepared using the Agilent SureSelect enriched the number of reads mapped by 3x-146x compared to samples enriched only with a poly(A)-enrichment and were consistently able to detect a greater number of genes, most of which were low abundance transcripts. Similarly, in the *A. fumigatus* comparisons, the poly(A)-enrichment by itself was unable to extract a sufficient number of *A. fumigatus* reads to accurately represent the transcriptome of the sample. When the poly(A)-enrichment was supplemented with Agilent SureSelect capture, the enrichment of *A. fumigatus* reads was increased 614-1,212x. When using the Agilent SureSelect instead of the rRNA-, poly(A)-depletion preparation for the *Wolbachia* endosymbiont *w*Bm transcriptome, the Agilent SureSelect samples were enriched for *w*Bm mapped reads by 20-41x in the gerbil life cycle samples and 353-2,242x in the vector life cycle samples.

For each of these samples, if the fold enrichment for the number of mapped reads in the poly(A)-enriched or total RNA Agilent SureSelect is plotted against the percentage of reads mapped in its poly(A)-enrichment or poly(A), rRNA depletion counterpart, the data follow a power law **(Figure 5)**. As expected, the fold enrichment obtained with the Agilent SureSelect capture is inversely proportional to the percentage of mapped reads obtained using the currently used enrichment methods of poly(A)-

441 enrichment to capture eukaryotic RNA or rRNA- and poly(A)-depletion to capture bacterial RNA from
442 multi-species samples, indicating samples with a lower relative abundance of RNA from the target
443 organism yield the greatest fold enrichment.
444 While the Agilent SureSelect can enrich a sample for transcripts of interest, the platform requires probes
445 designed for each gene to avoid any enrichment bias. Most instances of the Agilent SureSelect failing to
446 detect a gene that was detected in samples enriched using only the poly(A)-enrichment or rRNA-,
447 poly(A)-depletion was due to a lack of designed probes for the gene. Because the *B. malayi* annotation is
448 currently being updated, the baits were designed with an older annotation than the one used for
449 feature counting. Similarly, the bait design for *w*Bm was based on the annotation published by Foster et
450 *al* [18] while the annotation used for feature counting originated from GenBank (NC_006833.1). In both
451 cases, there were genes able to be detected with the poly(A)-enrichment or depletion, but not the
452 Agilent SureSelect. Additionally, several genes were observed to have significantly higher expression
453 values in the poly(A)-enrichment or rRNA, poly(A)-depletion samples compared to their Agilent
454 SureSelect counterpart.
455 These results illustrate the power and advantages of using probe-based enrichment to facilitate the
456 analysis of samples that are the most biologically relevant, like those in animal tissue at a biologically
457 relevant multiplicity of infection. The Agilent SureSelect platform serves as a method to extract reads
458 from a secondary or tertiary organism in a sample as well as to detect low abundance transcripts. Using
459 this platform, we successfully extracted a sufficient number of reads to represent the *B. malayi* and
460 *w*Bm transcriptomes in the vector portion of the *B. malayi* life cycle, the *A. fumigatus* transcriptome in a
461 mouse infection, and the *w*Bm transcriptome in the mammalian portion of the *B. malayi* life cycle.
462 Provided a transcriptome experiment has an adequate bait design, we believe the Agilent SureSelect
463 platform to be ideal and necessary in enriching samples for multi-species transcriptomic experiments,
464 especially those in which secondary organisms are of low abundance.

465

Acknowledgements

This project was funded by federal funds from the National Institute of Allergy and Infectious Diseases, National Institutes of Health, Department of Health and Human Services under grant number U19 AI110820.

Author Contributions

MC and JCDH wrote the manuscript. LT, HL, SL, NK, XZ, and REB performed sample preparation, library construction, capture experiments, and/or sequencing. MC and AS conducted bioinformatic data analysis. LJT, LS, CMF, DAR, JMF, VMB, and JCDH were involved in study design and data interpretation. SGF and MLM provided samples. All authors read, edited, and approved the manuscript.

Competing Financial Interests Statement

We have no competing financial interest.

Data availability

The data set(s) supporting the results of this article are available in the Sequence Read Archive (SRA) repository. The *B. malayi* datasets are available in SRP068692, the *w*Bm datasets are available in SRP068711, and the *A. fumigatus* datasets are available in PRJNA421149.

References

1. Naidoo S, Visser EA, Zwart L, Toit YD, Bhadauria V, Shuey LS: **Dual RNA-Sequencing to Elucidate the Plant-Pathogen Duel**. *Curr Issues Mol Biol* 2017, **27**:127-142.

2. Niemiec MJ, Grumaz C, Ermert D, Desel C, Shankar M, Lopes JP, Mills IG, Stevens P, Sohn K, Urban CF: **Dual transcriptome of the immediate neutrophil and Candida albicans interplay**. *BMC Genomics* 2017, **18**(1):696.

3. Li P, Xu Z, Sun X, Yin Y, Fan Y, Zhao J, Mao X, Huang J, Yang F, Zhu L: **Transcript profiling of the immunological interactions between Actinobacillus pleuropneumoniae serotype 7 and the host by dual RNA-seq**. *BMC Microbiol* 2017, **17**(1):193.

4. Bruno VM, Shetty AC, Yano J, Fidel PL, Jr., Noverr MC, Peters BM: **Transcriptomic analysis of vulvovaginal candidiasis identifies a role for the NLRP3 inflammasome**. *MBio* 2015, **6**(2).

5. Humphrys MS, Creasy T, Sun Y, Shetty AC, Chibucos MC, Drabek EF, Fraser CM, Farooq U, Sengamalay N, Ott S *et al*: **Simultaneous transcriptional profiling of bacteria and their host cells**. *PLoS One* 2013, **8**(12):e80597.

6. Hennessy RC, Glaring MA, Olsson S, Stougaard P: **Transcriptomic profiling of microbe-microbe interactions reveals the specific response of the biocontrol strain P. fluorescens In5 to the phytopathogen Rhizoctonia solani**. *BMC Res Notes* 2017, **10**(1):376.

7. Bing X, Attardo GM, Vigneron A, Aksoy E, Scolari F, Malacrida A, Weiss BL, Aksoy S: **Unravelling the relationship between the tsetse fly and its obligate symbiont Wigglesworthia: transcriptomic and metabolomic landscapes reveal highly integrated physiological networks**. *Proc Biol Sci* 2017, **284**(1857).

8. Camilios-Neto D, Bonato P, Wassem R, Tadra-Sfeir MZ, Brusamarello-Santos LC, Valdameri G, Donatti L, Faoro H, Weiss VA, Chubatsu LS *et al*: **Dual RNA-seq transcriptional analysis of wheat**

roots colonized by Azospirillum brasilense reveals up-regulation of nutrient acquisition and cell cycle genes. *BMC Genomics* 2014, **15**:378.

9. Grote A, Voronin D, Ding T, Twaddle A, Unnasch TR, Lustigman S, Ghedin E: **Defining Brugia malayi and Wolbachia symbiosis by stage-specific dual RNA-seq**. *PLoS Negl Trop Dis* 2017, **11**(3):e0005357.

10. Kumar N, Lin M, Zhao X, Ott S, Santana-Cruz I, Daugherty S, Rikihisa Y, Sadzewicz L, Tallon LJ, Fraser CM *et al*: **Efficient Enrichment of Bacterial mRNA from Host-Bacteria Total RNA Samples**. *Sci Rep* 2016, **6**:34850.

11. Amorim-Vaz S, Tran Vdu T, Pradervand S, Pagni M, Coste AT, Sanglard D: **RNA Enrichment Method for Quantitative Transcriptional Analysis of Pathogens In Vivo Applied to the Fungus Candida albicans**. *MBio* 2015, **6**(5):e00942-00915.

12. Sheppard DC, Rieg G, Chiang LY, Filler SG, Edwards JE, Jr., Ibrahim AS: **Novel inhalational murine model of invasive pulmonary aspergillosis**. *Antimicrob Agents Chemother* 2004, **48**(5):1908-1911.

13. Chiang LY, Sheppard DC, Gravelat FN, Patterson TF, Filler SG: **Aspergillus fumigatus stimulates leukocyte adhesion molecules and cytokine production by endothelial cells in vitro and during invasive pulmonary disease**. *Infect Immun* 2008, **76**(8):3429-3438.

14. Kumar N, Creasy T, Sun Y, Flowers M, Tallon LJ, Dunning Hotopp JC: **Efficient subtraction of insect rRNA prior to transcriptome analysis of Wolbachia-Drosophila lateral gene transfer**. *BMC Res Notes* 2012, **5**:230.

15. Trapnell C, Pachter L, Salzberg SL: **TopHat: discovering splice junctions with RNA-Seq**. *Bioinformatics* 2009, **25**(9):1105-1111.

16. Anders S, Pyl PT, Huber W: **HTSeq--a Python framework to work with high-throughput sequencing data**. *Bioinformatics* 2015, **31**(2):166-169.

17. Lagesen K, Hallin P, Rodland EA, Staerfeldt HH, Rognes T, Ussery DW: **RNAmmer: consistent and rapid annotation of ribosomal RNA genes**. *Nucleic Acids Res* 2007, **35**(9):3100-3108.

18. Foster J, Ganatra M, Kamal I, Ware J, Makarova K, Ivanova N, Bhattacharyya A, Kapatral V, Kumar S, Posfai J *et al*: **The *Wolbachia* genome of *Brugia malayi*: endosymbiont evolution within a human pathogenic nematode**. *PLoS Biol* 2005, **3**(4):e121.

19. Langmead B, Trapnell C, Pop M, Salzberg SL: **Ultrafast and memory-efficient alignment of short DNA sequences to the human genome**. *Genome Biol* 2009, **10**(3):R25.

20. Li H, Handsaker B, Wysoker A, Fennell T, Ruan J, Homer N, Marth G, Abecasis G, Durbin R, Genome Project Data Processing S: **The Sequence Alignment/Map format and SAMtools**. *Bioinformatics* 2009, **25**(16):2078-2079.

Figure Legends

Figure 1. Sample and library preparation

This schematic illustrates the sample (auburn rectangle) and library (blue rectangle) preparation workflow terminating in the libraries that were loaded on the Illumina sequencer. **(a)** For *B. malayi* and *A. fumigatus,* a poly(A)-selected sample was created from an aliquot of total RNA that was used to create a poly(A)-selected library. **(b)** The *B. malayi* or *A. fumigatus* Agilent SureSelect (AgSS) baits were subsequently used to capture the targeted RNA from poly(A)-selected libraries. **(c)** For AgSS-enriched *w*Bm libraries, an RNA library was constructed from an aliquot of total RNA that underwent targeted enrichment with the *Wolbachia* AgSS baits. Unlike the eukaryotic enrichments, the bacterial AgSS capture is performed on total RNA. For a limited number of libraries described in the text, an RNA library was constructed from an aliquot of total RNA (i.e. without poly(A)-enrichment) that underwent targeted enrichment with the *Brugia* AgSS baits. **(d)** For poly(A)/rRNA-depleted libraries enriched for *w*Bm, an aliquot of total RNA from either mosquito thoraces or adult nematodes was enriched for bacterial mRNA by removing Gram-negative and human rRNAs with two RiboZero removal kits and polyadenylated RNAs with DynaBeads.

Figure 2. Comparison of the poly(A)-enriched to the poly(A)-enriched Agilent SureSelect *B. malayi* transcriptomes from 18 hpi, 4 dpi, and 8 dpi vector life stages

(a) A principal component analysis (PCA) plot was generated using the $\log_2$ TPM values for the poly(A)-enriched only (circles) and poly(A)-enriched Agilent SureSelect (triangles) *B. malayi* from 18 hpi (red), 4 dpi (green), and 8 dpi (blue) vector samples. The size of each symbol denotes the number of reads mapped to protein-coding genes for each sample. The samples cluster based on *B. malayi* sample rather than by the enrichment method, indicating the poly(A)-enriched Agilent SureSelect does not substantially differ from its poly(A)-enrichment only counterpart in representing the *B. malayi* transcriptome for the shown samples. Samples with the lowest number of reads (e.g. the 18 hpi

564 samples) cluster further from their replicates than expected, likely attributed to an insufficient number
565 of reads and indicating that enrichment is most desirable in these situations. **(b)** For each sample, the
566 $\log_2$ TPM values for genes in the poly(A)-enriched Agilent SureSelect samples were plotted against the
567 $\log_2$ TPM values for genes in the poly(A)-enrichment only samples when expression was observed with
568 both enrichment methods for the sample. Genes with similar expression in the Agilent SureSelect and
569 the poly(A)-enrichment samples are expected to lie close to the identity line (x=y; red). Genes whose
570 expression values are more elevated in the poly(A)-enriched Agilent SureSelect sample compared to the
571 poly(A)-enrichment sample lie below the identity line while genes more elevated in the poly(A)-
572 enrichment compared to the poly(A)-enriched Agilent SureSelect lie above the identity line. **(c)** For all
573 genes expressed using both enrichment methods for each sample, the frequency distribution of the $\log_2$-
574 transformed ratio of the poly(A)-enriched Agilent SureSelect TPM to the poly(A) enrichment TPM was
575 plotted. Genes with $\log_2$ ratio values >0 have higher expression values in the poly(A)-enriched Agilent
576 SureSelect sample while $\log_2$ ratio values <0 are representative of genes with higher expression values
577 with the poly(A) enrichment. Significantly biased genes were defined as those differentiating by >3
578 standard deviations (red) from the mean of the $\log_2$-transformed ratio values (red). Across each
579 comparison, the number of genes with significantly elevated expression in the Agilent SureSelect
580 comprised at most 0.31% of the total number of *B. malayi* protein-coding genes while the number of
581 genes with significantly elevated expression in the poly(A)-enrichment samples comprised at most
582 1.52% of *B. malayi* protein-coding genes.

583 **Figure 3. Comparison of the rRNA-, poly(A)-depleted to the total RNA Agilent**
584 **SureSelect *w*Bm transcriptomes from the female 24 dpi and adult *B. malayi* life**
585 **stages**

586 **(a)** A principal component analysis of the rRNA-, poly(A)-depleted (triangle) and total RNA Agilent
587 SureSelect (circle) *w*Bm transcriptome from three samples of the *B. malayi* gerbil life stage was
588 conducted, with one sample from female 24 dpi *B. malayi* (red) and two samples from adult female *B.*

589 *malayi* (blue). The size of each point is relative to the number of reads mapped to protein-coding genes
590 for each sample. In this instance, the samples no longer cluster based on the sample type. Instead, the
591 samples distinctly cluster apart based on enrichment method, most likely due to the smaller number of
592 reads present in samples lacking the Agilent SureSelect capture. Consistent with this, the sample with
593 the fewest reads, one of the rRNA-, poly(A)-depleted adult females, is most distant. The three samples
594 enriched using the Agilent SureSelect cluster together, possibly indicating the similarity of *w*Bm
595 transcriptomes originating from female 24 dpi and adult *B. malayi*. **(b)** For each sample, the $\log_2$ TPM
596 values for genes detected with the Agilent SureSelect capture on total RNA were plotted against the $\log_2$
597 TPM values for genes detected with the rRNA-, poly(A)-depletion when a gene was detected in both
598 enrichments. Genes with similar expression in both the total RNA Agilent SureSelect and the rRNA-,
599 poly(A)-depleted samples are expected to lie close to the identity line (x=y; red). Genes whose
600 expression values are more elevated in the total RNA Agilent SureSelect compared to the rRNA-, poly(A)-
601 depletion lie below the identity line while genes more elevated in the rRNA-, poly(A)-depletion
602 compared to the total RNA Agilent SureSelect lie above the identity line. **(c)** The frequency distribution
603 $\log_2$-transformed ratio of the total RNA Agilent SureSelect TPM to the rRNA- and poly(A)-depleted TPM
604 for each gene detected in both enrichment methods was plotted. The blue, dashed line indicates the
605 mean $\log_2$-transformed ratio while the red dashed line marks two standard deviations from the mean
606 $\log_2$-transformed ratio. Genes with $\log_2$ ratio values >2 standard deviations above or below the mean
607 were marked as biased towards the rRNA-, poly(A)-depletion, total RNA Agilent SureSelect or the rRNA-,
608 poly(A)-depletion, respectively. Across all 9 comparisons, an average of ~2.9 genes were detected with
609 significantly higher expression with the total RNA Agilent SureSelect while an average of ~7.1 genes had
610 significantly higher expression in the rRNA-, poly(A)-depleted samples.

Figure 4. Comparison of the poly(A)-enriched Agilent SureSelect to the total RNA Agilent SureSelect *B. malayi* transcriptomes from 18 hpi and 8 dpi vector life stages

(a) For both the 18 hpi and 8 dpi vector samples, the $\log_2$ TPM values for each *B. malayi* gene detected in both the poly(A)-enriched Agilent SureSelect and the total RNA Agilent SureSelect were plotted against one another. Most genes in both plots fall along the identity line (y=x; red), indicating their similar expression values in both the poly(A)-enriched Agilent SureSelect and the total RNA Agilent SureSelect libraries. **(b)** A histogram of the $\log_2$ ratios of the poly(A)-enriched Agilent SureSelect TPM to the total RNA Agilent SureSelect TPM was generated for each sample using all genes detected with both enrichment methods. The blue dashed line marks the average $\log_2$ ratio value while the red lines mark three standard deviations from the average $\log_2$ ratio. Genes with $\log_2$ ratio values >3 standard deviations above the average are marked as significantly elevated in the poly(A)-enriched Agilent SureSelect while genes with $\log_2$ ratio values >3 standard deviations below the average are marked as significantly elevated in the total RNA Agilent SureSelect samples. For both the library preparations, ≤1.4% (155 genes) of protein-coding genes are biased towards a single enrichment method, indicating no significant bias towards an enrichment.

Figure 5. Scatter plot of the percentage of poly(A)-enrichment or depletion reads mapped against the fold enrichment value observed using the Agilent SureSelect follows a power law

The fold enrichment value for each sample used in the poly(A)-enrichment/depletion versus Agilent SureSelect comparisons for *B. malayi* (red), *A. fumigatus*(blue), and *w*Bm (green) was calculated by taking the ratio of the percentage of Agilent SureSelect reads mapped to the percentage of poly(A)-enrichment/depletion reads mapped. The relationship between these fold enrichment values and the percentage of the poly(A)-enrichment/depletion reads mapped to the reference genome can be fitted to a power law. The inversely proportional relationship between the Agilent SureSelect fold enrichment values and the percentage of reads mapped using the percentage of reads mapped using the poly(A)-

637 enrichment/depletion indicates that the fold enrichment conferred using the Agilent SureSelect

638 platform exponentially increases with the exponential decrease of the percentage of reads mapped

639 using the standard enrichment/depletion methods until an ~1300-fold enrichment.

640

Supplementary Files

Supplementary Table 1: RNA-Seq statistics for poly(A)-enriched Agilent SureSelect and poly(A)-enrichment libraries from *B. malayi* samples collected following infection of the mosquito vector

Supplementary Table 2: RNA-Seq statistics for Agilent SureSelect and poly(A)-enrichment libraries from *A. fumigatus*

Supplementary Table 3: RNA-Seq statistics for Agilent SureSelect and rRNA-, poly(A)-depletion libraries from *w*Bm

Supplementary Table 4: RNA-Seq statistics for *B. malayi* transcriptome data using Agilent SureSelect with total RNA or poly(A)-enriched RNA

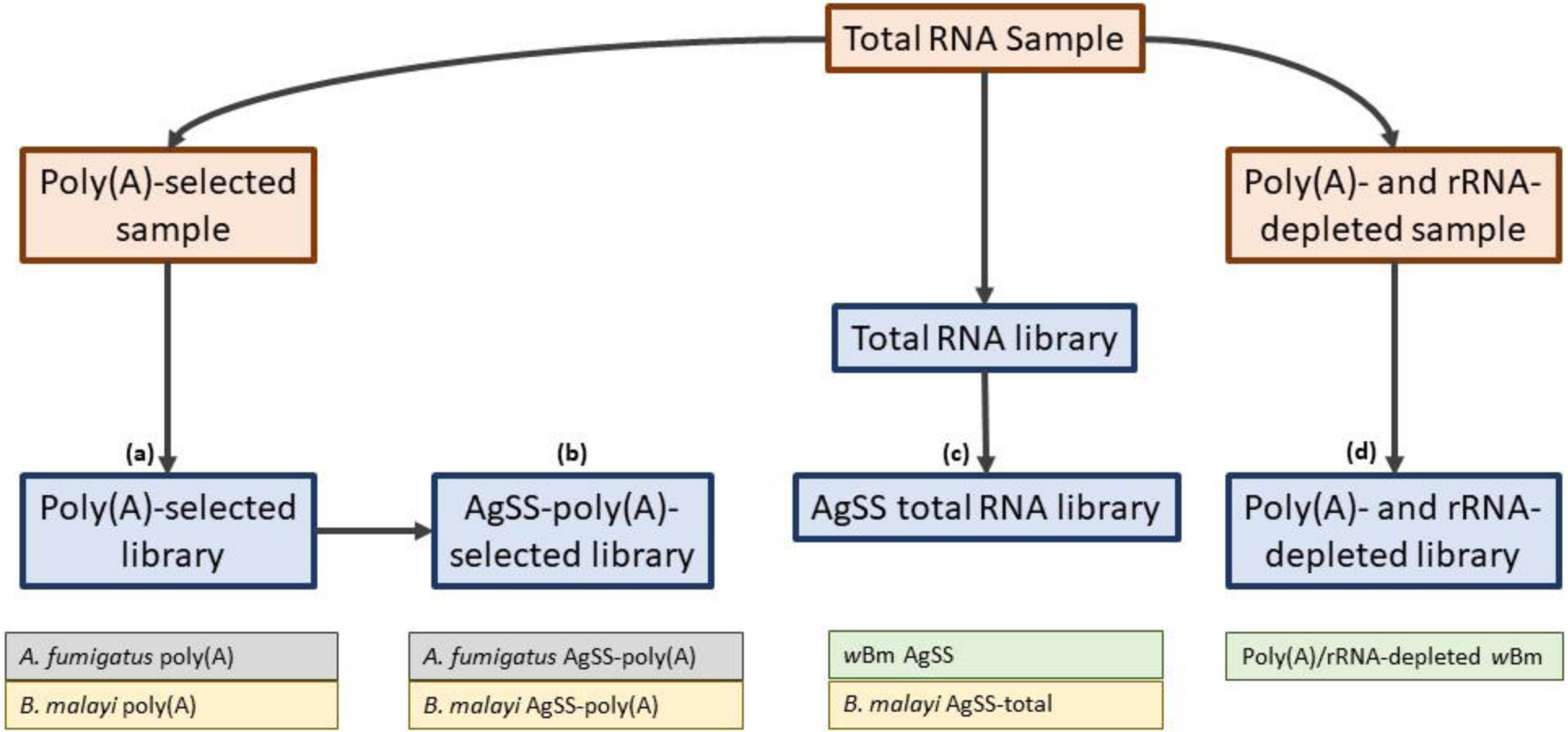

Target Organism	Method 1	Method 2	Comparsion	Sample type
Brugia	Poly(A)-selected	AgSS-poly(A)-selected	Poly(A) v. AgSS-poly(A)	Mosquito thoraces & Adult worms
Aspergillus	Poly(A)-selected	AgSS-poly(A)-selected	Poly(A) v. AgSS-poly(A)	Mouse tissue
Wolbachia	Poly(A)/rRNA-depleted	AgSS-total	Poly(A)/rRNA-depleted v. AgSS-total	Mosquito thoraces & Adult worms
Brugia	AgSS-poly(A)-selected	AgSS-total	AgSS-poly(A) v. AgSS-total	Mosquito thoraces

A

PC2

50

0

−50

−100

0

100

PC1

B. malayi Samples

18 hpi, vector

4 dpi, vector

8 dpi, vector

Library Preparation

Poly(A)−enriched Agilent SureSelect

Poly(A)−enrichment

Reads Mapped to Features

5.0e+07

1.0e+08

1.5e+08

B

B. malayi : 18 hpi, vector

B. malayi : 4 dpi, vector

B. malayi : 8 dpi, vector

$y = 1.9 + 0.66 \cdot x$, $r^2 = 0.559$

$y = 0.53 + 0.88 \cdot x$, $r^2 = 0.853$

$y = 0.57 + 0.88 \cdot x$, $r^2 = 0.867$

$y = 1.4 + 0.75 \cdot x$, $r^2 = 0.703$

$y = 0.58 + 0.88 \cdot x$, $r^2 = 0.848$

$y = 0.66 + 0.86 \cdot x$, $r^2 = 0.855$

$\log_2$TPM poly (A) − enrichment

$\log_2$TPM poly (A) − enriched Agilent SureSelect

C

B. malayi : 18 hpi, vector

B. malayi : 4 dpi, vector

B. malayi : 8 dpi, vector

number of genes

$\log_2$(TPM poly (A) − enriched Agilent SureSelect/TPM poly (A) − enrichment)

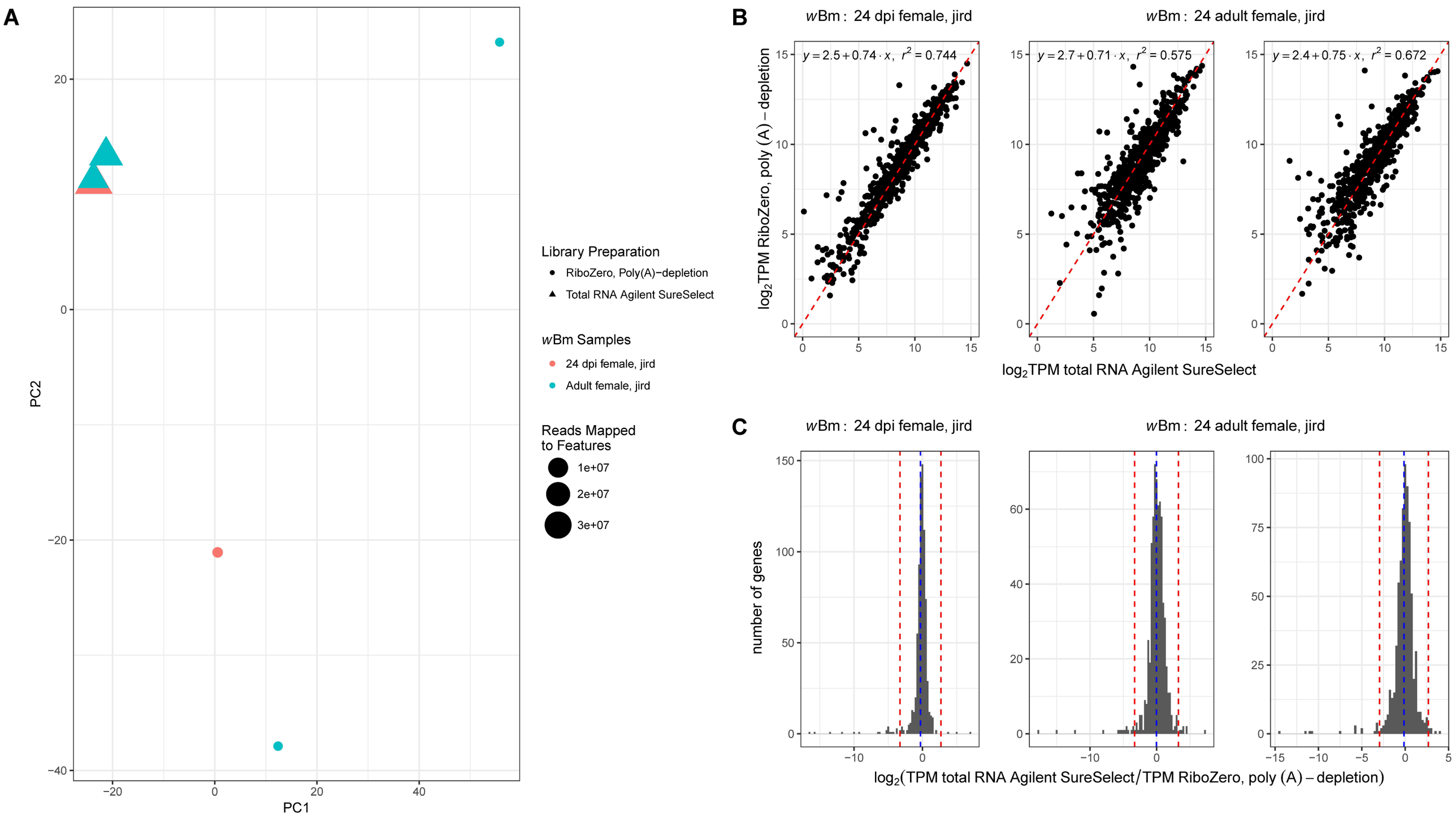
A
PC2
PC1
20
0
−20
−40
−20
0
20
40
Library Preparation
RiboZero, Poly(A)−depletion
Total RNA Agilent SureSelect
wBm Samples
24 dpi female, jird
Adult female, jird
Reads Mapped to Features
1e+07
2e+07
3e+07
B
wBm : 24 dpi female, jird
wBm : 24 adult female, jird
y = 2.5 + 0.74 · x, r2 = 0.744
y = 2.7 + 0.71 · x, r2 = 0.575
y = 2.4 + 0.75 · x, r2 = 0.672
log2TPM RiboZero, poly (A) − depletion
log2TPM total RNA Agilent SureSelect
C
wBm : 24 dpi female, jird
wBm : 24 adult female, jird
number of genes
log2(TPM total RNA Agilent SureSelect/TPM RiboZero, poly (A) − depletion)

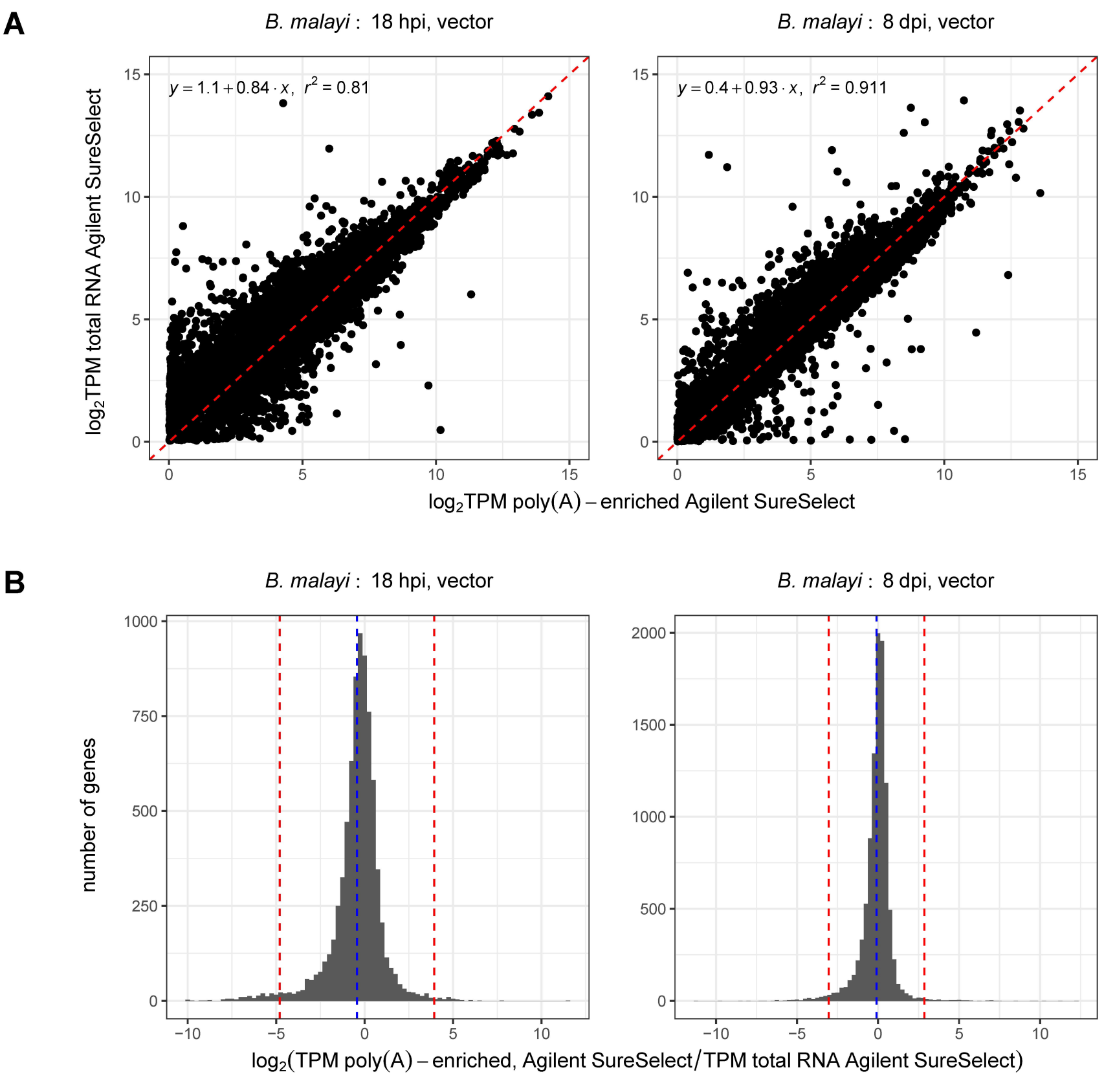
A
B. malayi : 18 hpi, vector
B. malayi : 8 dpi, vector
y = 1.1 + 0.84 · x, r² = 0.81
y = 0.4 + 0.93 · x, r² = 0.911
log2TPM total RNA Agilent SureSelect
log2TPM poly(A) – enriched Agilent SureSelect
B
B. malayi : 18 hpi, vector
B. malayi : 8 dpi, vector
number of genes
log2(TPM poly(A) – enriched, Agilent SureSelect/TPM total RNA Agilent SureSelect)

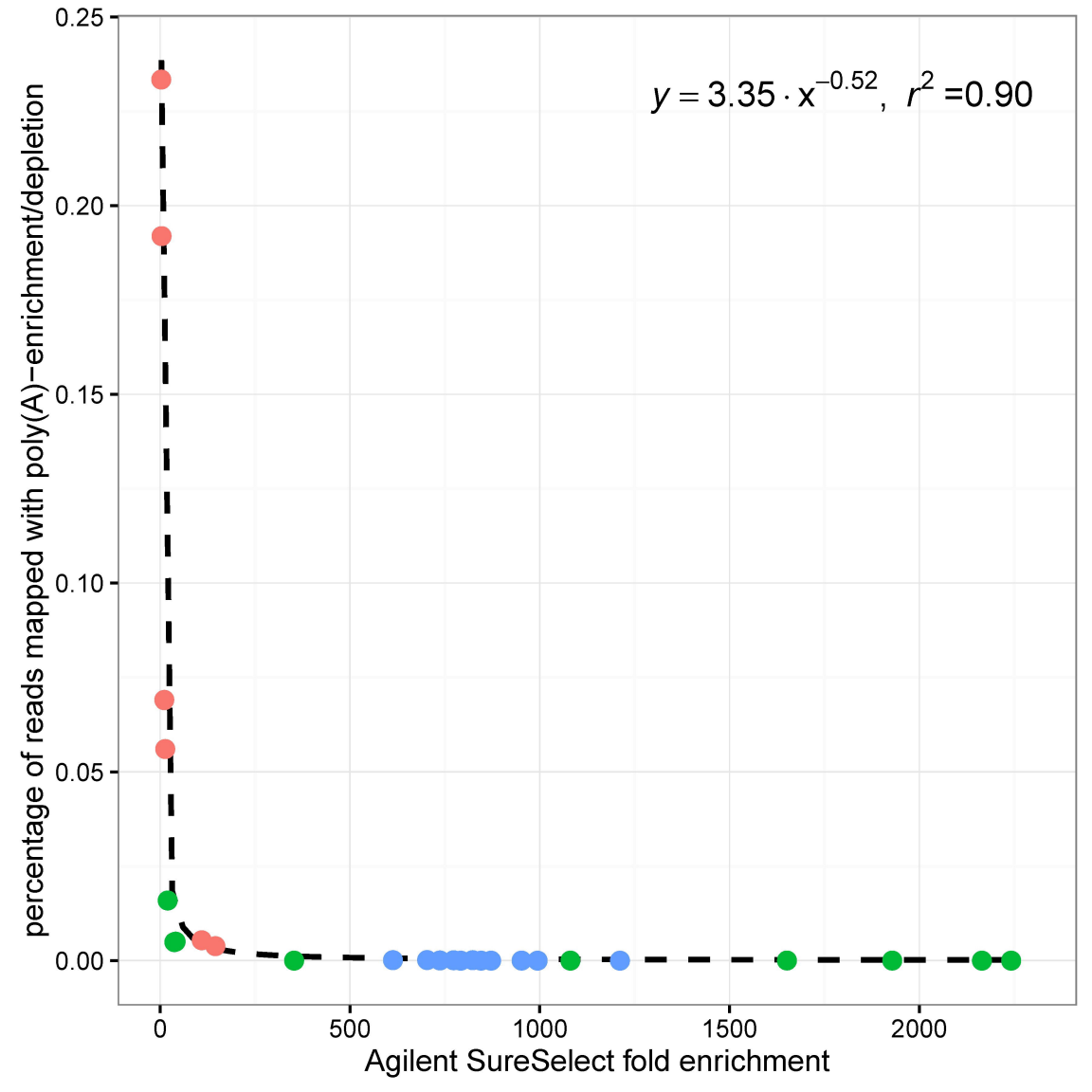
$y = 3.35 \cdot x^{-0.52}$, r^2 =0.90
percentage of reads mapped with poly(A)−enrichment/depletion
0.25
0.20
0.15
0.10
0.05
0.00
0
500
1000
1500
2000
Agilent SureSelect fold enrichment